Landes Bioscience www.landesbioscience.com

# Supplemental Material to:

Liqin Du, Robert Borkowski, Zhenze Zhao, Xiuye Ma, Xiaojie Yu, Xian-Jin Xie, Alexander Pertsemlidis

## A high-throughput screen identifies miRNA inhibitors regulating lung cancer cell survival and response to paclitaxel

2013; 10(11)
http://dx.doi.org/10.4161/rna.26541

www.landesbioscience.com/journals/rnabiology/article/26541/

Addendum:

1. 2013RNABIOL0096R1-SupTable1.xlsx

**Supplementary Material**

**Supplementary Figure 1. Experimental design for the HTS screens.** The inhibitors, each of which targets one human miRNA, were arrayed in a one-inhibitor–one-well format on 96-well plates. Cells were reverse-transfected with the library oligos. After 72 h, cells were treated with paclitaxel at the $IC_{50}$ for each cell line. After 48 h of incubation with paclitaxel, cell viability was measured by quantifying the ATP concentration produced by living cells. The raw measurements of cell viability were normalized to the mean of the central 60 wells of each plate to permit plate-to-plate comparisons. Each miRNA inhibitor was assigned three numbers, its effect on cell viability in the absence ($V_{carrier}$) or presence of paclitaxel ($V_{paclitaxel}$), and a sensitivity ratio (S) calculated as viability in paclitaxel divided by viability in the absence of drug ($S = V_{paclitaxel}/V_{carrier}$). miRNA inhibitors in the tails of the distribution identified as potent regulators of viability or paclitaxel response of the lung cancer cell lines.

**Supplementary Figure 2. Dose-dependent cytotoxicity curves for paclitaxel in cell lines H1993, H1155 and H358.** Cells were treated with different concentrations of paclitaxel for three days. Cell viability was then measured as described above. The $IC_{50}$ for each cell line was derived by non-linear regression with a variable slope inhibitory dose-response model.

**Supplementary Figure 3. Distributions of z scores for the effects of individual miRNA inhibitors on cell viability and paclitaxel response. (A-F)** The quantile-quantile plots compare the observed z scores with those expected from a standard normal distribution. The observed scores deviate significantly from normality and exhibit an excess of large values corresponding to screen hits.

**Supplementary Figure 4. Expression levels of miR-133a/b, miR-361-3p and miR-346 in a panel of lung cancer cell lines.** Expression levels of **(A)** miR-133a, **(B)** miR-133b, **(C)** miR-346 and **(D)** miR-361-3p levels were measured using miRNA expression arrays. Shown are the relative expression levels of the miRNAs in the indicated cell lines.

**Supplementary Table 1. miRNA inhibitors identified as having general effects on lung cancer cell survival and response to paclitaxel using 20% and 30% thresholds.**

**Supplementary Table 2. $IC_{50}$ values for cytotoxicity of the three miRNA inhibitors derived from dose-response analysis.** Shown are the cell line names and the $IC_{50}$s and 95% confidence intervals (CI) associated with each miRNA inhibitor.

**Supplementary Table 3. Genetic backgrounds of cell lines used in this study**. Shown are the cell line names, tumor sub-types from which the cell lines are derived, ages and genders of the patients, and identified mutations in TP53, CDKN2A and KRAS.

**Supplementary Table 4. Cell cycle distribution of G1 phase-synchronized cells treated with miR-133a/b and miR-361-3p inhibitors.**

**References**


1. Bluemn EG, Spencer ES, Mecham B, Gordon RR, Coleman I, Lewinshtein D, et al. PPP2R2C loss promotes castration-resistant prostate cancer growth and is associated with increased prostate cancer-specific mortality. Mol Cancer Res 2013.
2. Barcelo-Coblijn G, Martin ML, de Almeida RF, Noguera-Salva MA, Marcilla-Etxenike A, Guardiola-Serrano F, et al. Sphingomyelin and sphingomyelin synthase (SMS) in the malignant transformation of glioma cells and in 2-hydroxyoleic acid therapy. Proc Natl Acad Sci U S A 2011; 108:19569-74.
3. Huang J, Yan J, Zhang J, Zhu S, Wang Y, Shi T, et al. SUMO1 modification of PTEN regulates tumorigenesis by controlling its association with the plasma membrane. Nat Commun 2012; 3:911.
4. Marin MB, Ghenea S, Spiridon LN, Chiritoiu GN, Petrescu AJ, Petrescu SM. Tyrosinase degradation is prevented when EDEM1 lacks the intrinsically disordered region. PLoS One 2012; 7:e42998.
5. Li Y, Li W, Yang Y, Lu Y, He C, Hu G, et al. MicroRNA-21 targets LRRFIP1 and contributes to VM-26 resistance in glioblastoma multiforme. Brain Res 2009; 1286:13-8.
6. Jiang Z, Guo J, Xiao B, Miao Y, Huang R, Li D, et al. Increased expression of miR-421 in human gastric carcinoma and its clinical association. J Gastroenterol 2010; 45:17-23.
7. Zhang YJ, Wei L, Liu M, Li J, Zheng YQ, Gao Y, et al. BTG2 inhibits the proliferation, invasion, and apoptosis of MDA-MB-231 triple-negative breast cancer cells. Tumour Biol 2013.
8. Madan E, Gogna R, Kuppusamy P, Bhatt M, Pati U, Mahdi AA. TIGAR induces p53-mediated cell-cycle arrest by regulation of RB-E2F1 complex. Br J Cancer 2012; 107:516-26.
9. Zhang S, Jiang T, Feng L, Sun J, Lu H, Wang Q, et al. Yin Yang-1 suppresses differentiation of hepatocellular carcinoma cells through the downregulation of CCAAT/enhancer-binding protein alpha. J Mol Med (Berl) 2012; 90:1069-77.
10. Caldeira J, Simoes-Correia J, Paredes J, Pinto MT, Sousa S, Corso G, et al. CPEB1, a novel gene silenced in gastric cancer: a Drosophila approach. Gut 2012; 61:1115-23.
11. Zhang Z, Xu Z, Wang X, Wang H, Yao Z, Mu Y, et al. Ectopic Ikaros expression positively correlates with lung cancer progression. Anat Rec (Hoboken) 2013.
12. Choi HS, Bode AM, Shim JH, Lee SY, Dong Z. c-Jun N-terminal kinase 1 phosphorylates Myt1 to prevent UVA-induced skin cancer. Mol Cell Biol 2009; 29:2168-80.
13. auf dem Keller U, Huber M, Beyer TA, Kumin A, Siemes C, Braun S, et al. Nrf transcription factors in keratinocytes are essential for skin tumor prevention but not for wound healing. Mol Cell Biol 2006; 26:3773-84.
14. Feng W, Marquez RT, Lu Z, Liu J, Lu KH, Issa JP, et al. Imprinted tumor suppressor genes ARHI and PEG3 are the most frequently down-regulated in human ovarian cancers by loss of heterozygosity and promoter methylation. Cancer 2008; 112:1489-502.
15. Harada N, Yokoyama T, Yamaji R, Nakano Y, Inui H. RanBP10 acts as a novel coactivator for the androgen receptor. Biochem Biophys Res Commun 2008; 368:121-5.
16. Zhang Y, Yang Y, Yeh S, Chang C. ARA67/PAT1 functions as a repressor to suppress androgen receptor transactivation. Mol Cell Biol 2004; 24:1044-57.
17. Yu SJ, Hu JY, Kuang XY, Luo JM, Hou YF, Di GH, et al. MicroRNA-200a Promotes Anoikis Resistance and Metastasis by Targeting YAP1 in Human Breast Cancer. Clin Cancer Res 2013; 19:1389-99.
18. Wong JS, Iorns E, Rheault MN, Ward TM, Rashmi P, Weber U, et al. Rescue of tropomyosin deficiency in Drosophila and human cancer cells by synaptopodin reveals a role of tropomyosin alpha in RhoA stabilization. EMBO J 2012; 31:1028-40.
19. Sun H, Jiang L, Luo X, Jin W, He Q, An J, et al. Potential tumor-suppressive role of monoglyceride lipase in human colorectal cancer. Oncogene 2013; 32:234-41.
20. Niu X, Zhang T, Liao L, Zhou L, Lindner DJ, Zhou M, et al. The von Hippel-Lindau tumor suppressor protein regulates gene expression and tumor growth through histone demethylase JARID1C. Oncogene 2012; 31:776-86.

21. Williams YN, Masuda M, Sakurai-Yageta M, Maruyama T, Shibuya M, Murakami Y. Cell adhesion and prostate tumor-suppressor activity of TSLL2/IGSF4C, an immunoglobulin superfamily molecule homologous to TSLC1/IGSF4. Oncogene 2006; 25:1446-53.

# Suppl. Figure 1

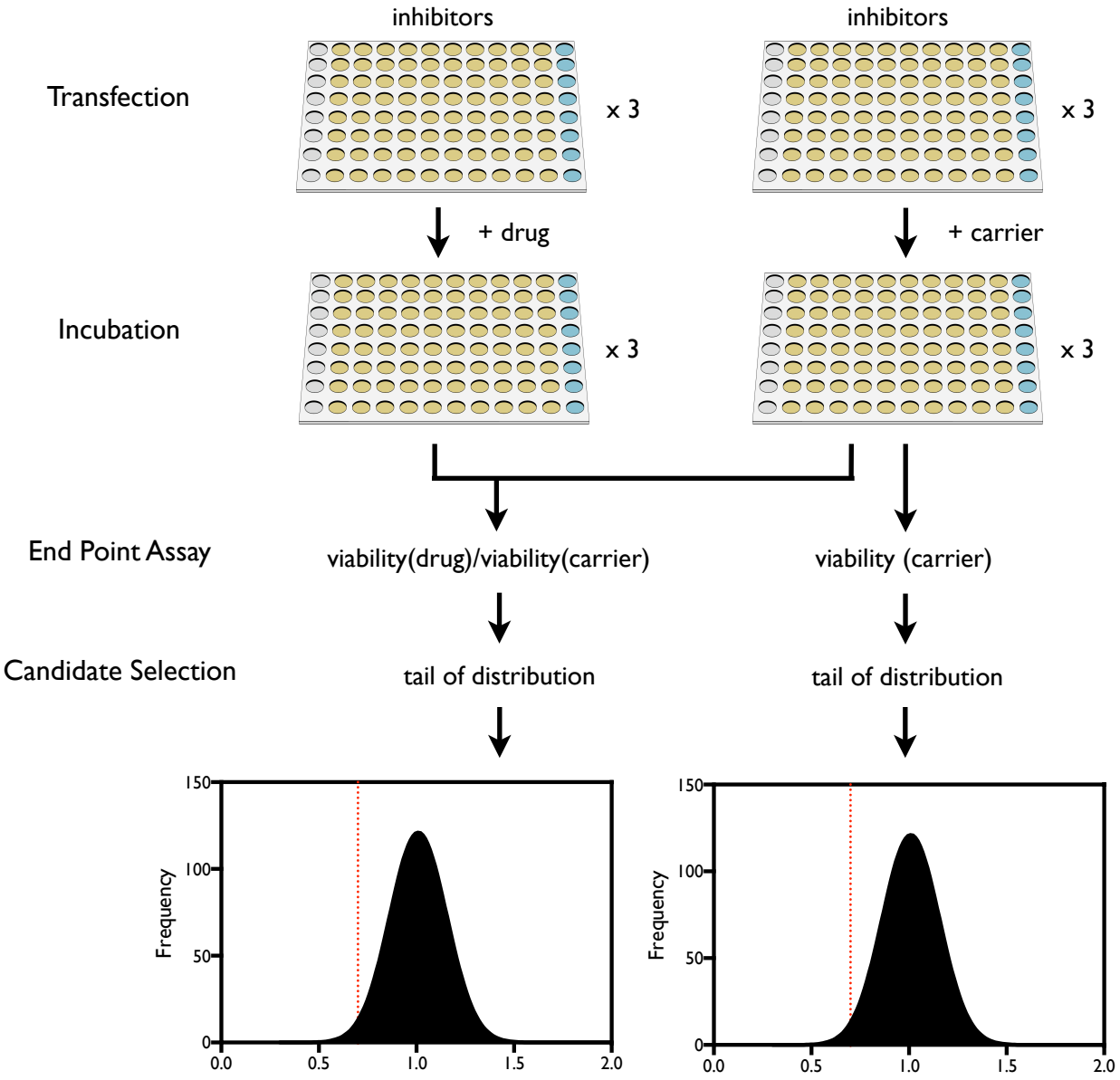

Supplementary Figure 2

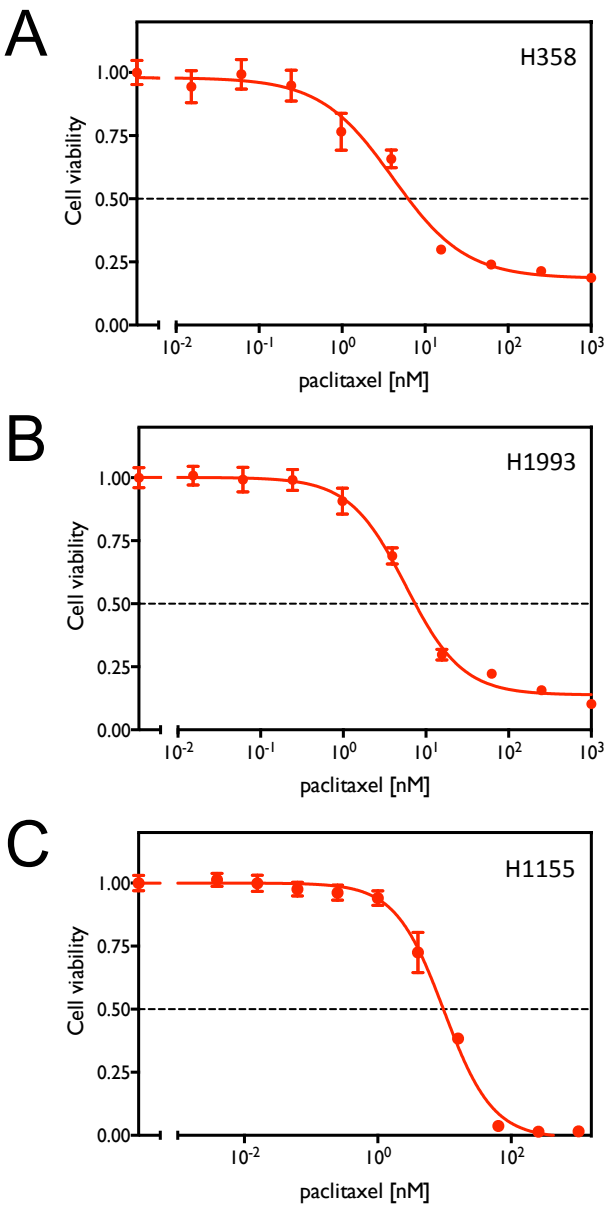

Supplementary Figure 3

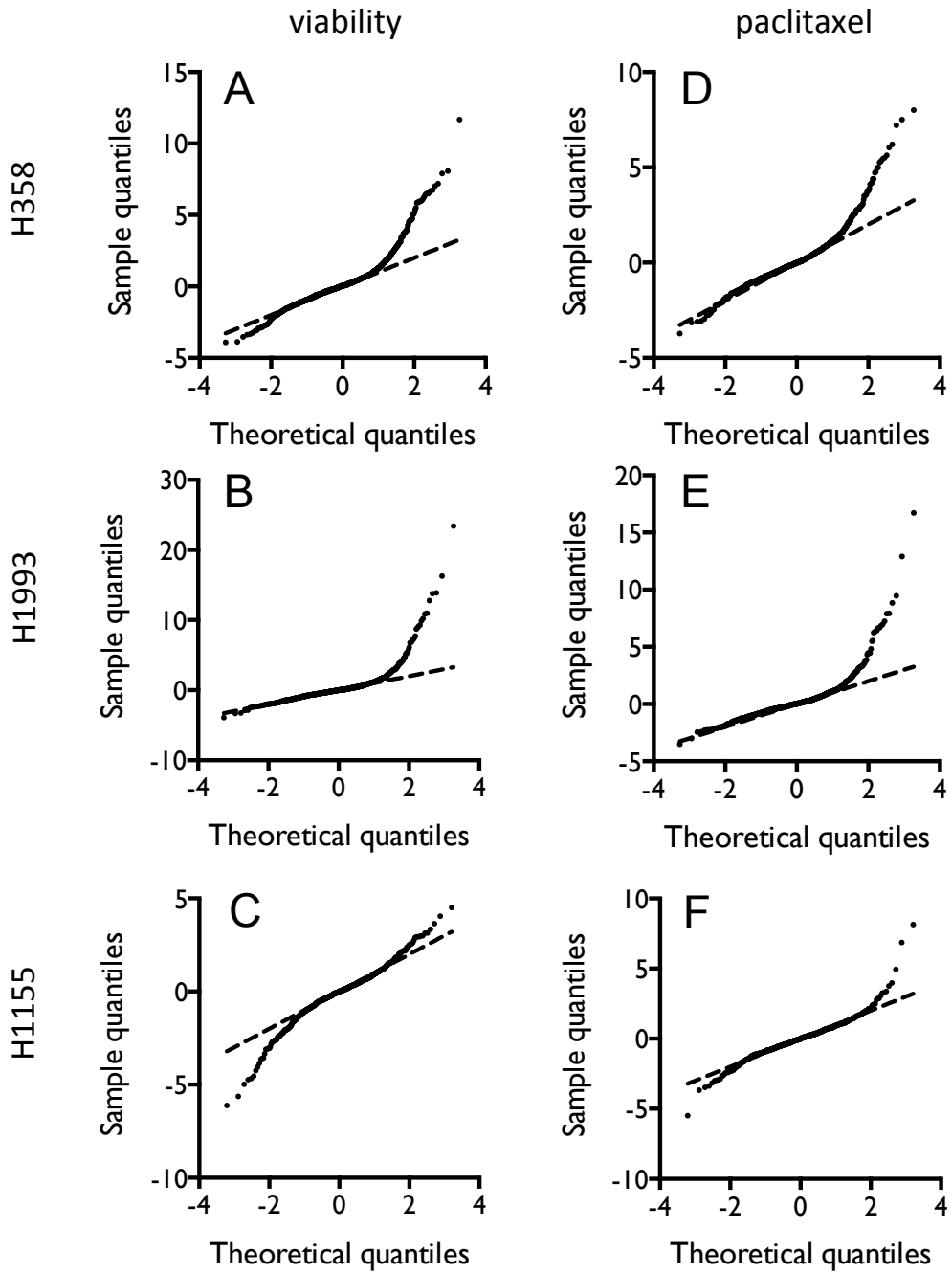

Supplementary Figure 4

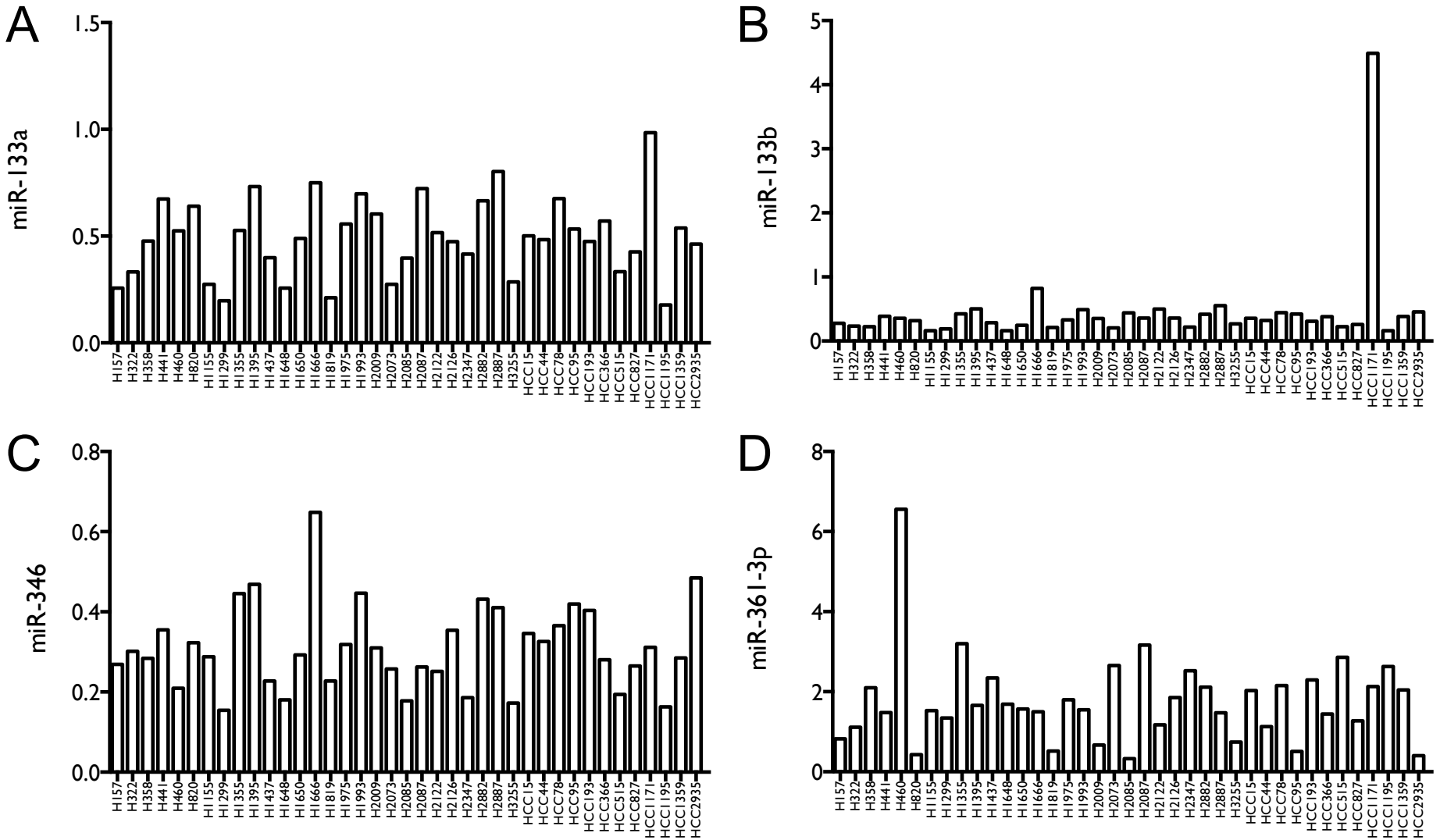

**Supplementary Table 2.**

| Cell Line | miR-133a/b inh $IC_{50}$ (95% CI) | miR-346 inh $IC_{50}$ (95% CI) | miR-361-3p inh $IC_{50}$ (95 %CI) |
|---|---|---|---|
| H1993 | 4.60 (4.34-4.88) | 16.62 (14.15-20.06) | 13.59 (11.83-15.84) |
| H157 | 2.74 (2.53-2.96) | 8.05 (7.22-9.03) | 4.91 (4.34-5.57) |
| H1299 | 4.07 (3.84-4.32) | 6.68 (6.27-7.13) | 5.72 (5.43-6.01) |
| H1819 | 26.13 (22.93-30.10) | 41.21 (33.87-50.85) | 42.05 (36.14-49.17) |
| HCC95 | 10.49 (9.36-11.88) | 73.85 (52.24- ) | 11.65 (10.51-12.95) |
| HCC2450 | 16.95 (14.01-20.98) | 21.45 (18.52-25.43) | 24.69 (20.37-30.63) |

**Supplementary Table 3.**

| Cell Line | Tumor Subtype | Age | Gender | TP53 | CDKN2A | KRAS |
|---|---|---|---|---|---|---|
| H358 | Adenocarcinoma | | M | WT | WT | G12V |
| H1819 | Adenocarcinoma | 55 | F | WT | WT | WT |
| H1993 | Adenocarcinoma | 47 | F | C242W | WT | WT |
| H1155 | Large Cell Neuroendocrine | 36 | M | R273H | WT | Q61H |
| H1299 | Large Cell Neuroendocrine | 43 | M | WT | WT | WT |
| H157 | Squamous Cell Carcinoma | 59 | M | E298* | E69* | G12R |
| HCC95 | Squamous Cell Carcinoma | 65 | M | WT | del | WT |
| HCC2450 | Squamous Cell Carcinoma | 52 | M | WT | WT | WT |

**Supplementary Table 4**

| | | 0h | 2h | 4h | 6h | 8h | 10h |
|---|---|---|---|---|---|---|---|
| | G1 | 44.1 | 47.6 | 10.9 | 14.4 | 20.5 | 23.4 |
| scrambled inh | S | 48.3 | 45.8 | 84.1 | 78.5 | 74.2 | 36.4 |
| | G2 | 6.4 | 4.4 | 8.8 | 6.6 | 3.3 | 39.5 |
| | G1 | 46.1 | 46.2 | 25.4 | 7.9 | 11 | 18.4 |
| miR-133a/b inh | S | 50.3 | 48.1 | 73.2 | 85.1 | 80.8 | 56.4 |
| | G2 | 1.3 | 6.2 | 5.3 | 5.7 | 6.5 | 23.4 |
| | G1 | 47.6 | 55 | 10.3 | 11.5 | 10.6 | 12.3 |
| miR-361-3p inh | S | 42.6 | 45.2 | 85.4 | 80 | 80.5 | 76 |
| | G2 | 7.3 | 0.3 | 7.1 | 7.2 | 7 | 9.1 |